Supplementary Information

# Molecular-scale visualization of sarcomere contraction within native cardiomyocytes

Laura Burbaum†, Jonathan Schneider†, Sarah Scholze, Ralph T Böttcher, Wolfgang Baumeister, Petra Schwille, Jürgen M Plitzko, Marion Jasnin*

† These authors contributed equally to this work

* Correspondence to: jasnin@biochem.mpg.de (M.J.)

**This PDF file includes:**

Supplementary Figures 1-9

Supplementary Tables 1-2

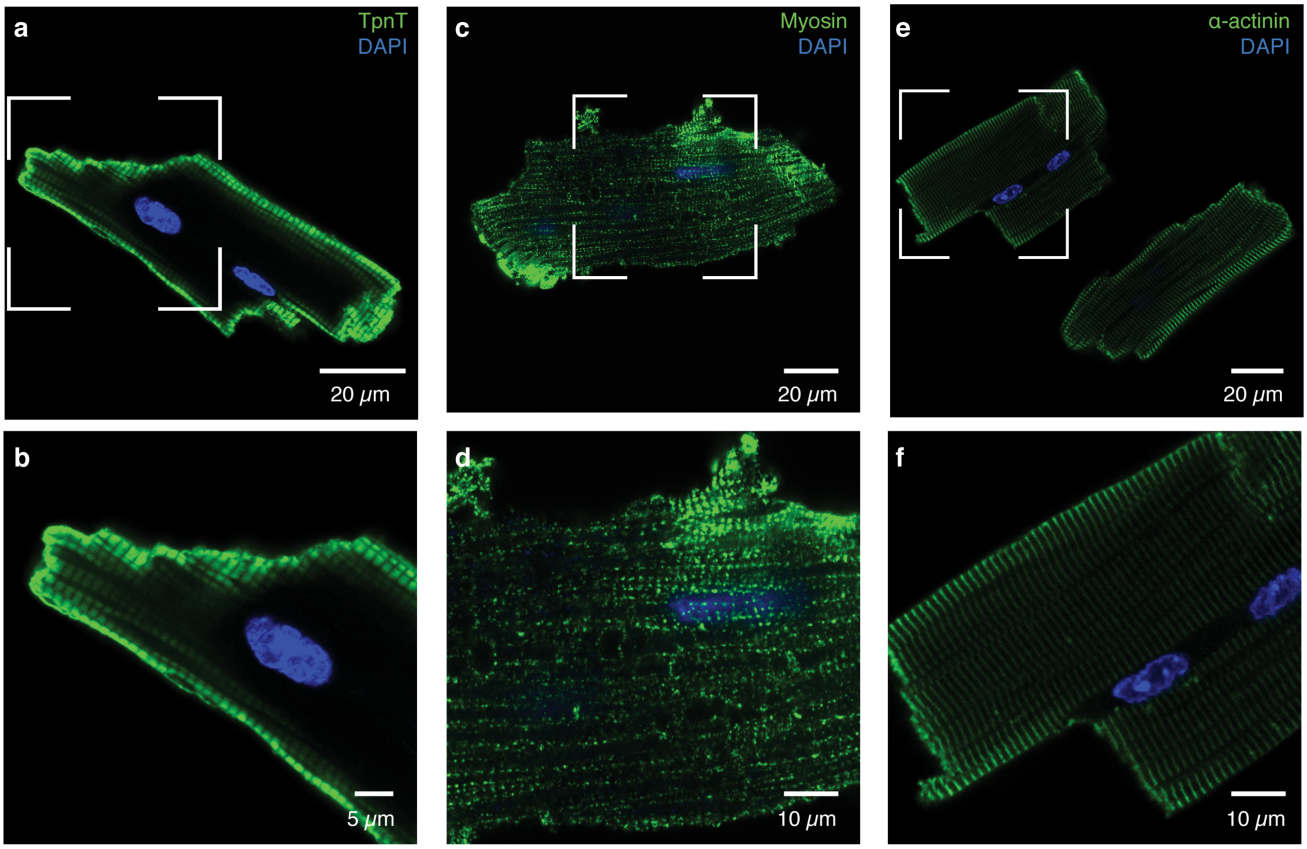


**Supplementary Fig. 1 | Myofibrillar organization in adult mouse cardiomyocytes at the microscale. a-f** The cells were labelled with antibodies specific for troponin T (TpnT, **a**, **b**), the heavy chain of myosin (Myosin, **c**, **d**) and α-actinin (**e**, **f**), respectively. Thin (**a**, **b**) and thick (**c**, **d**) filaments of adult mouse cardiomyocytes assemble into myofibrils, which are compactly arranged along the main axis of the rod-shaped cells. Myofibrils display regularly spaced Z-disks (**e**, **f**) with a sarcomere length of 1.5 ± 0.1 μm. This sarcomere length is not directly comparable with that of the neonatal cardiomyocytes since cells were isolated from different species. **b**,**d**,**f** Zoomed-in views of the framed regions in **a**, **c**, **e**, respectively. Each experiment was repeated independently at least 3 times with similar results.

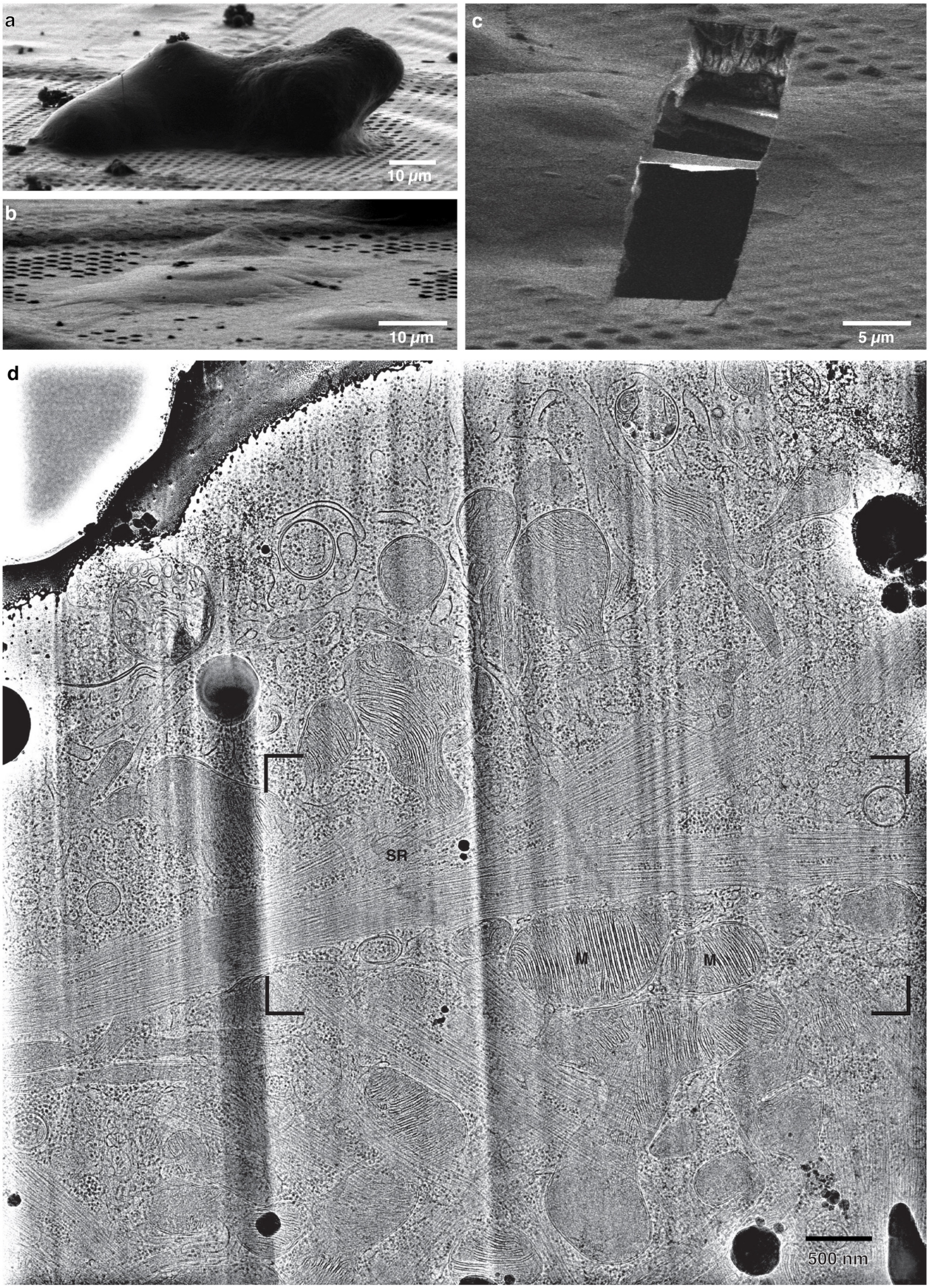
a
10 μm
b
10 μm
c
5 μm
d
SR
M
M
500 nm

**Supplementary Fig. 2 | Cryo-FIB sample preparation of neonatal rat cardiomyocytes for cryo-ET imaging. a** Scanning electron microscope (SEM) image of a frozen-hydrated adult mouse cardiomyocyte on an EM grid. Vitrification by plunge-freezing is not suitable for these cells because their thickness is larger than 10 µm. **b** Neonatal rat cardiomyocytes are thin, allowing optimal vitrification by plunge-freezing without the need for cryoprotectant. **c** 200-nm-thick lamella prepared in a plunge-frozen neonatal rat cardiomyocyte and imaged by FIB-induced secondary electrons. **d** Full TEM image of a neonatal cardiomyocyte lamella containing the cropped part shown in Fig. 2a. SR, sarcoplasmic reticulum; M, mitochondrion. A total of 8 lamellas prepared from 8 cells was used in this study. Each cell comes from 2 separate experiments in which 4 organisms were mixed and can therefore be considered as a biological replicate. Representative images are shown.

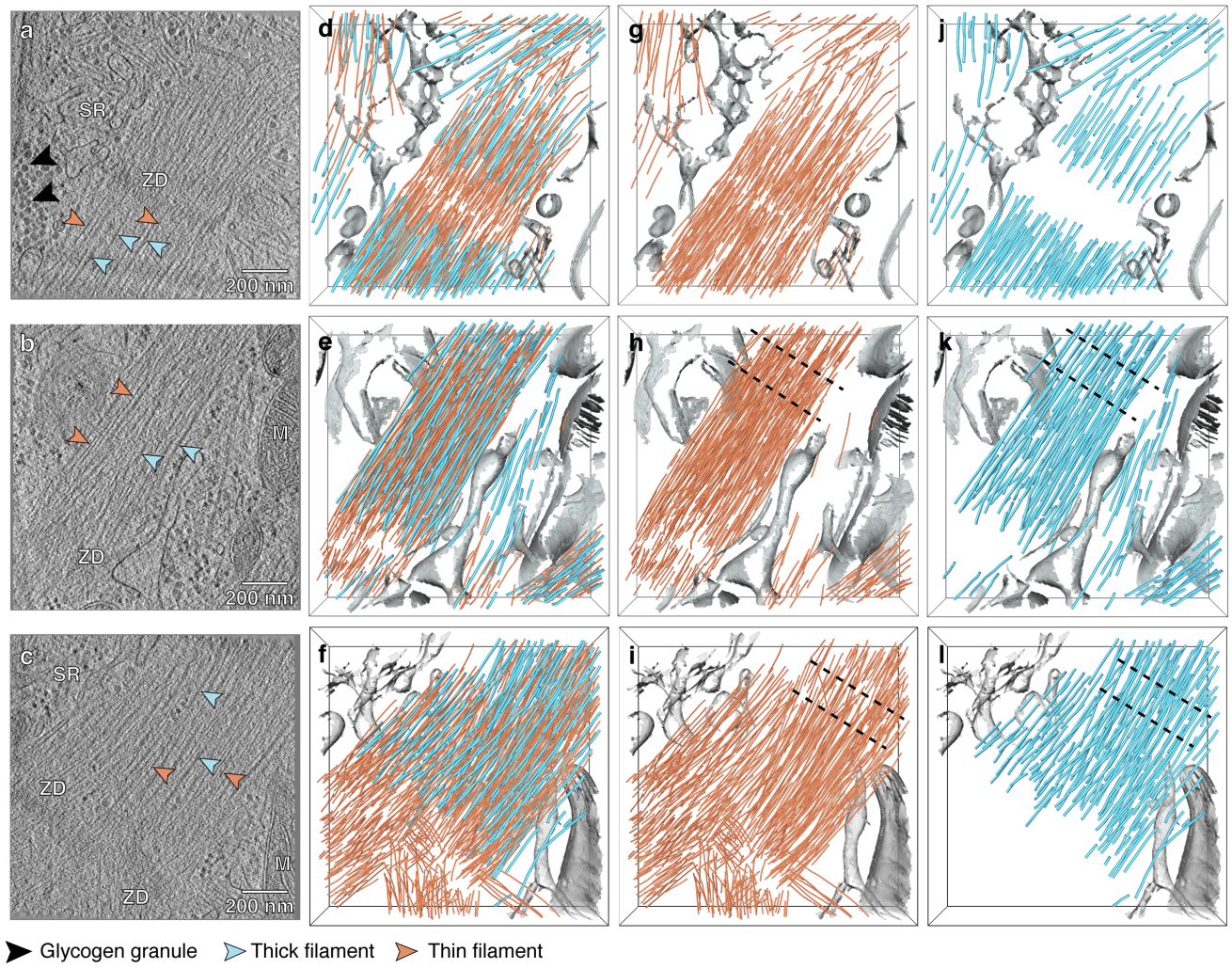


**Supplementary Fig. 3 | Nanoscale sarcomere organization revealed by *in situ* cryo-ET. a-c** 6.84 nm-thick slices from defocused tomographic volumes acquired in 3 different frozen-hydrated neonatal rat cardiomyocytes, revealing the myofibrillar environment. ZD, Z-disk; M, mitochondrion; SR, sarcoplasmic reticulum. **d-l** Corresponding 3D segmentation of the cellular volumes, showing the nanoscale organization of the thin (orange; **d-i**) and thick (cyan; **d-f**, **j-l**) filaments within unperturbed sarcomeres. Putative myosin bare zones estimated for an average sarcomere length of 1.8 µm are delineated by dashed black lines in **h**, **i**, **k**, **l**. A total of 13 tomograms acquired from 8 cells were used in this study (Supplementary Table 1). Each cell comes from 2 separate experiments in which 4 organisms were mixed and can therefore be considered as a biological replicate. Representative images are shown.

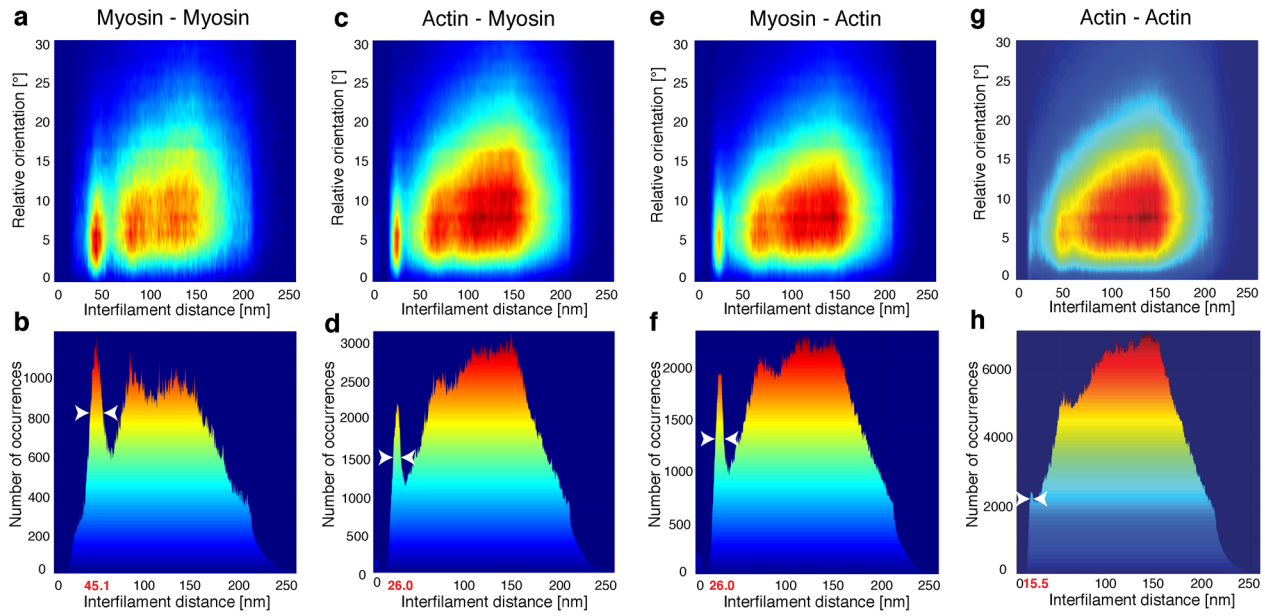


**Supplementary Fig. 4 | Near-neighbor analysis of myofilaments in neonatal rat cardiomyocytes. a**,**c**,**e**,**g** 2D histogram of interfilament distances and relative orientations between thick filaments (Myosin; **a**), between thick and thin filaments (Actin; **c**, **e**) and between thin filaments (**g**); **b**,**d**,**f**,**h** the corresponding histograms showing the number of occurrences of the interfilament distances. For each point along a filament, the closest point of each neighboring filament is characterized by its distance, $d$, and relative orientation, $\theta$, with respect to the reference point. The occurrences of ($d$, $\theta$) are represented in these 2D histograms, for filaments of the same type (that is, only thick filaments (**a**) or only thin filaments (**g**)) as well as for filaments of one type relative to the other (that is, neighboring thick filaments for the thin filaments (**c**), and reciprocally (**e**)). The peak occurring at the shortest interfilament distances and small $\theta$ (below 10°) in **a**, **c**, **e**, **g** corresponds to the contribution of the nearest parallel filaments. White arrowheads in **b**, **d**, **f**, **h** indicate the distance range for nearest parallel filaments, obtained from the distances with a number of occurrences higher than two third of the peak maximum. Thick filaments have an interfilament spacing of about 45.1 nm (**a**, **b**) and are found at about 26.0 nm from the thin filaments (**c**-**f**). Thin filaments have their nearest actin neighbors at about 15.5 nm (**g**, **h**).

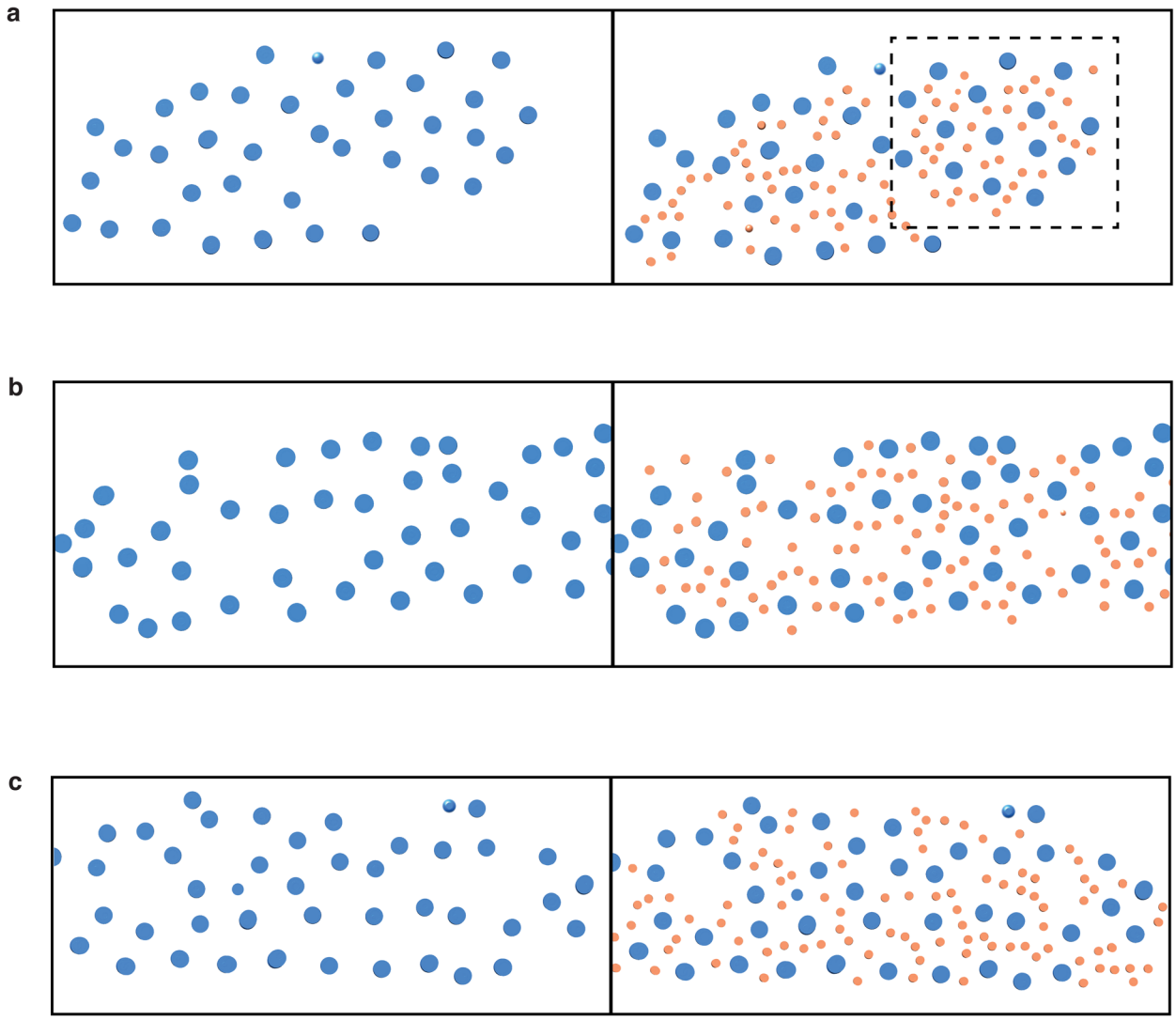


**Supplementary Fig. 5 | Examples of cross-sections through myofibrils of neonatal rat cardiomyocytes in the single-overlap region of the A-band. a-c** Thick filaments (blue) are hexagonally packed and surrounded by thin filaments (orange, right) at the trigonal positions of the lattice and outside of them. The framed area in (**a**) is shown in Fig. 3i. The slices were obtained from the myofibrils shown in Supplementary Fig. 3e, k (**a**), Fig. 2e, g (**b**) and Supplementary Fig. 3f, l (**c**).

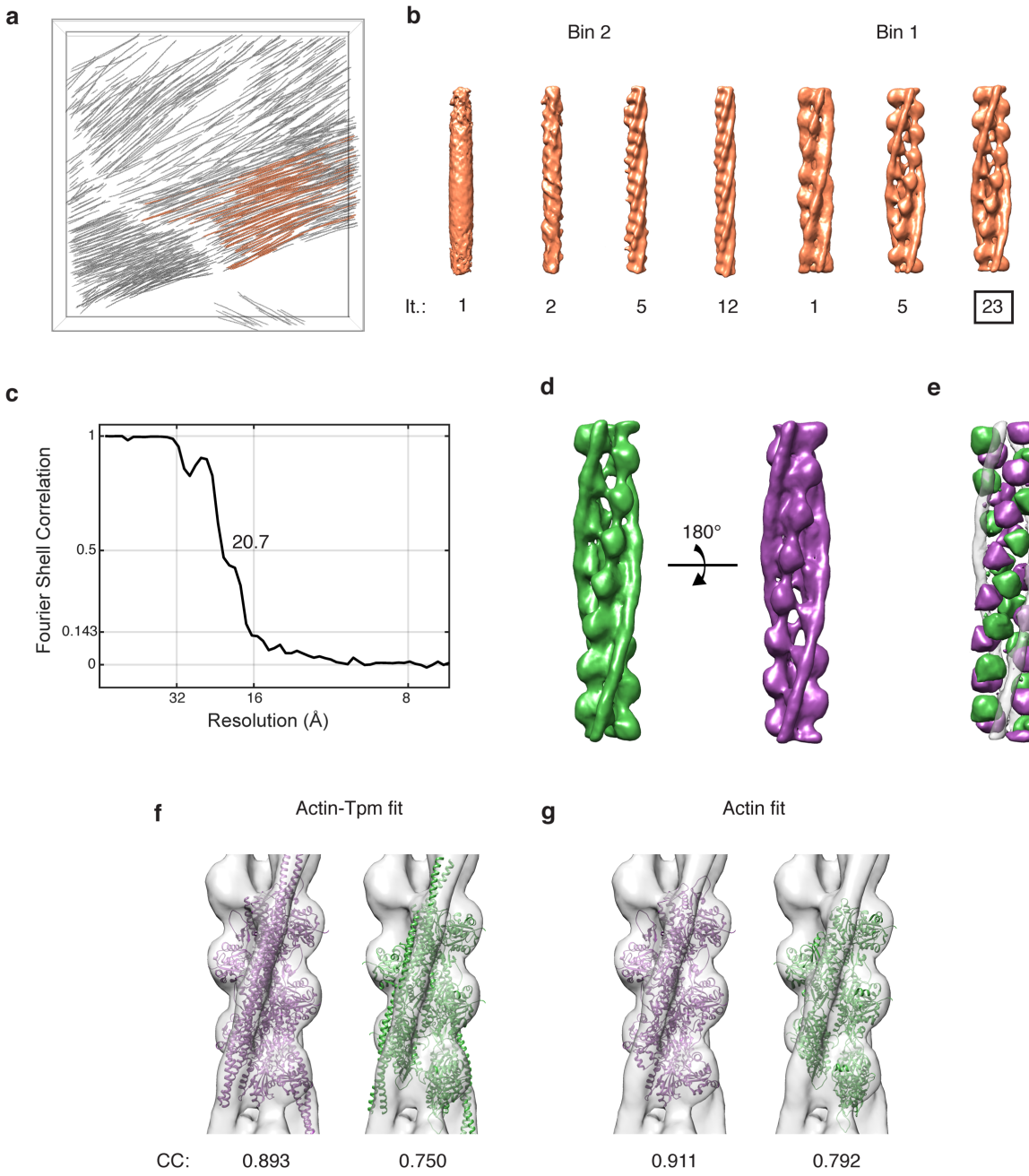


**Supplementary Fig. 6 | *De novo* structure generation from cryo-ET data of cardiac thin filaments. a** Thin filaments (orange) from the tomogram shown in Fig. 2b and Supplementary Movie 2 used for the generation of a *de novo* reference. **b** Iterative alignment using 2x binned (Bin 2) and unbinned (Bin 1) data resulted in the emergence of the helical pattern of the thin filament and yielded a structure of F-actin in complex with Tpm resolved at 20.7 Å. It, Iteration number. **c** Corresponding Fourier shell correlation plot. Since the data was not processed using gold-standard refinement, a cutoff of 0.5 was used. **d** Filament structures in opposite orientations (green and purple, respectively) and aligned on the Tpm densities. **e** Respective difference maps with superimposed Tpm densities (grey) revealing the actin positions associated to each polarity with respect to the Tpm. **f**, **g** Both orientations (same color code as in **d**) of the pseudoatomic model of the F-actin-Tpm complex (pdb 5jlh) docked into the *in situ* map (grey) shown in purple in **d** (**f**), and corresponding fits using the actin densities only (**g**). The cross-correlation (CC) results permitted to allocate the barbed (+) and pointed (-) end of the *de novo* F-actin structure (Fig. 4a).

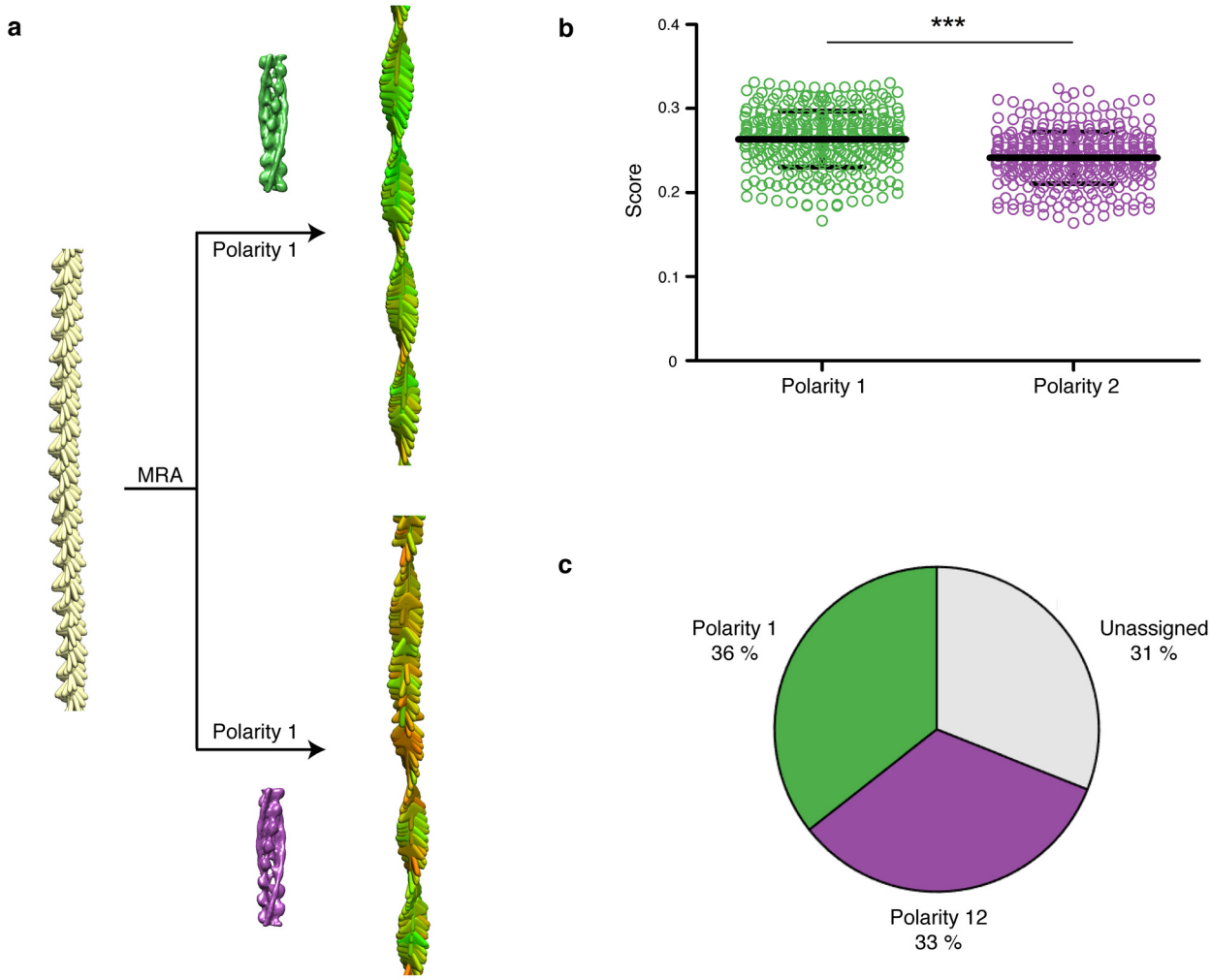


**Supplementary Fig. 7 | Workflow for the polarity assessment of the thin filaments imaged by cryo-ET. a** Multireference alignment (MRA) procedure applied to one filament with oversampled positions aligned along the *z*-axis and in-plane randomization represented by yellow arrows (left). Each position is aligned independently against a reference of each polarity (in green and purple, respectively), resulting in refined orientations and scores (high scores, green; low scores, red; right). Refinement against the green structure (Polarity 1) leads to uniform helical pattern, whereas alignment against the purple structure (Polarity 2) yields irregularities in the helical pattern. **b** Corresponding scores obtained for the single filament with n=333 independent sampling points for each polarity, with the mean and standard deviation indicated. Unpaired, 2-sided Student's t-test revealed significant differences between both polarities (***: $p < 0.001$). **c** Pie chart representing the results of the polarity assignment for the entire dataset of 594,317 subvolumes with $p < 0.05$. Source data are provided as a Source Data file.

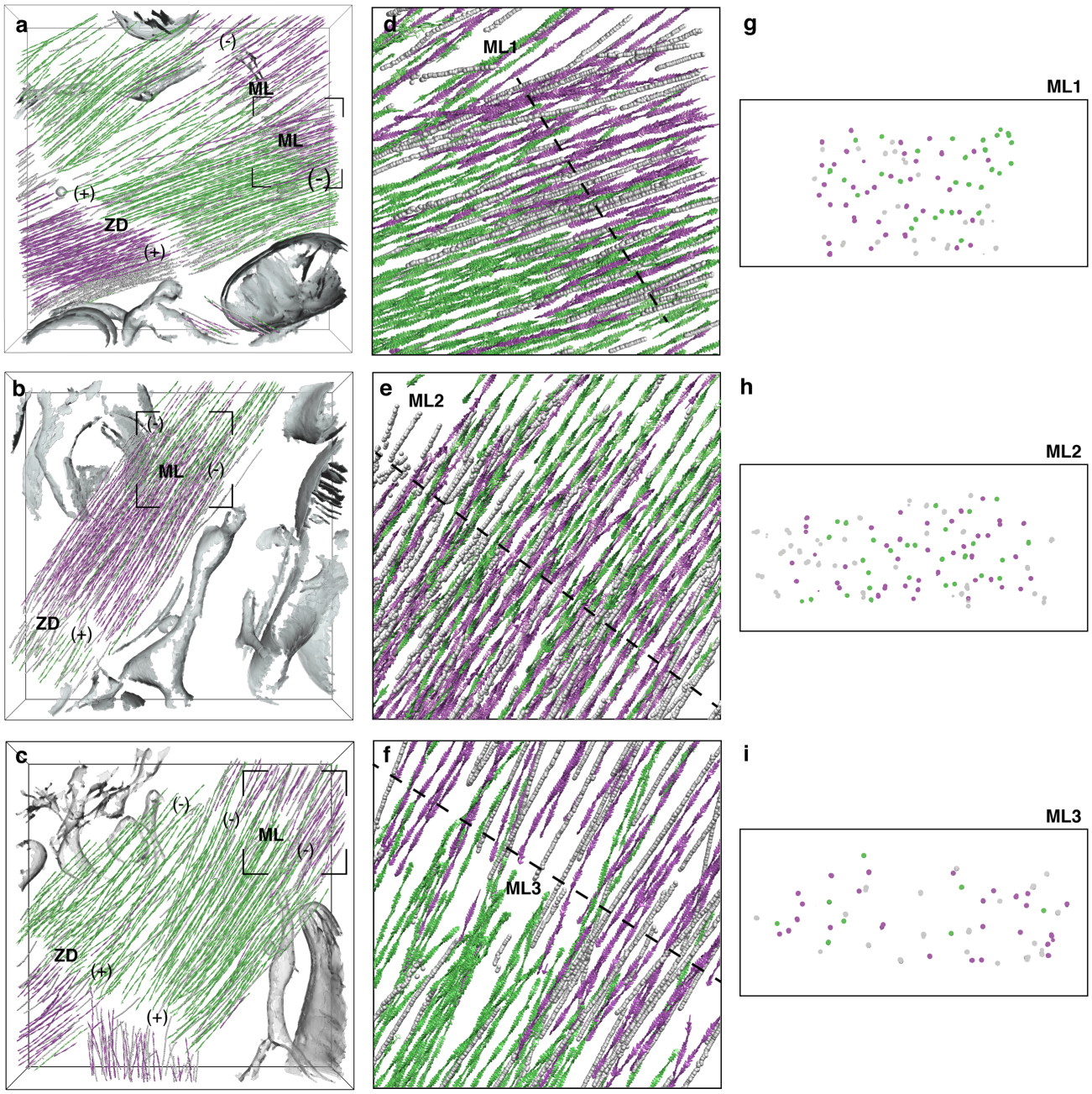


**Supplementary Fig. 8 | Polarity assignment and packing of neonatal cardiac thin filaments at the center of the sarcomere. a-c** Same examples as in Fig. 4 showing the unassigned filaments in grey, which correspond to 23% of the subvolumes in these datasets. Thin filaments with assigned polarity are represented by colored arrows pointing toward the pointed (-) end. ZD, Z-disk; ML, M-line. **d-f** Zoomed-in views of the framed regions in **a-c**, respectively, showing the thin filament orientations in the framed M-lines (ML1-3). **g-i** Cross-sections through ML1-3 at the locations indicated by the dotted lines in **d-f**.

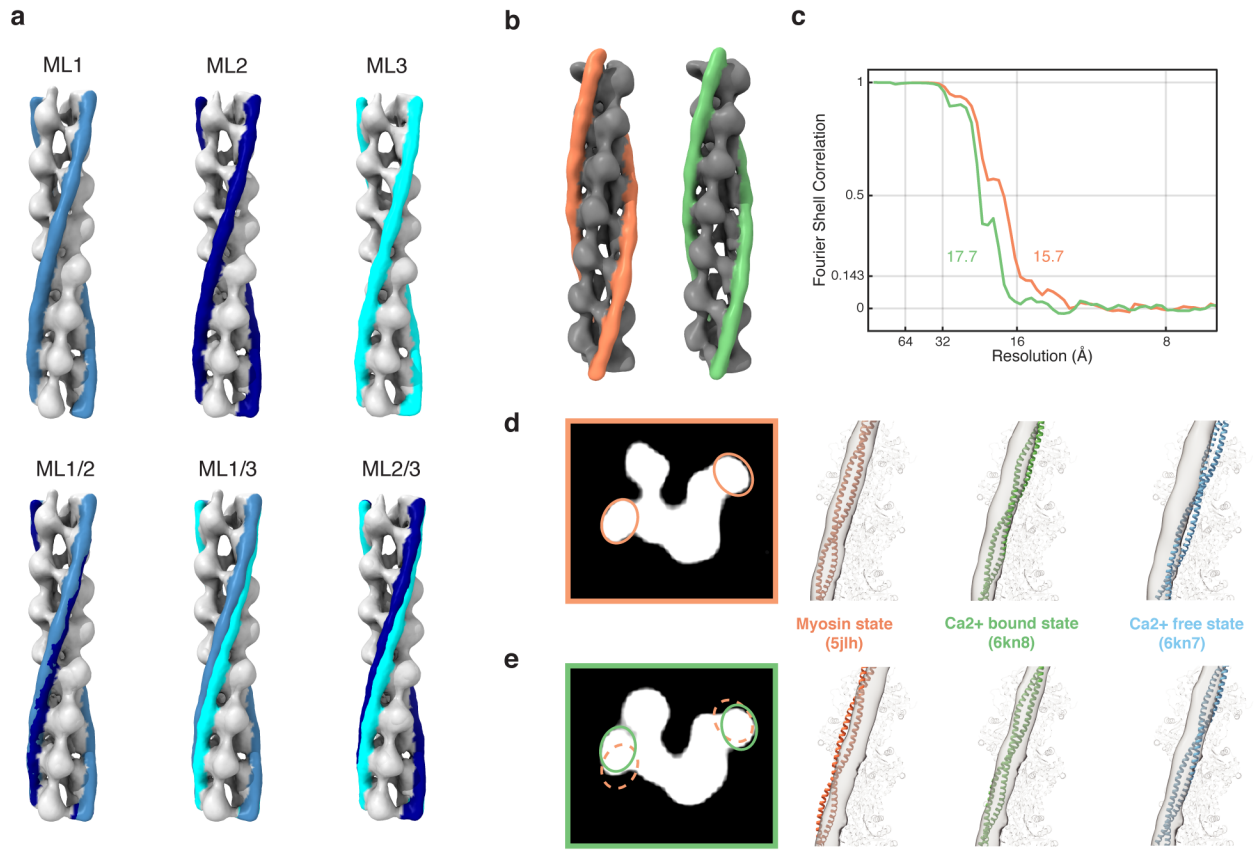


**Supplementary Fig. 9 | Resolution and functional state of the native cardiac thin filament structures. a** Subtomogram averages of the cardiac thin filament obtained from the data shown in Fig. 4b-d (ML1-3; blue, dark blue and cyan Tpm densities, respectively). Superposing ML1 and ML2 (ML1/2) reveals that these structures are similar. Superposing ML1 or ML2 with ML3 (ML1/3 and ML2/3, respectively) shows that the Tpm density is azimuthally shifted in ML3. **b** Final subtomogram averages associated with the wide (orange Tpm) and narrow (green Tpm) overlap at the M-lines. **c** Gold-standard FSC plots of the subtomogram averages shown in **b** with curves of the same color as the Tpm densities. **d-e** *x-y* slices through the 15.7 Å (**d**) and 17.7 Å (**e**) resolution structures shown in **b**, in which the Tpm densities are highlighted in orange and green, respectively, and close up into the fits of the pseudoatomic models in different states into the maps.

**Supplementary Table 1 | Data acquisition parameters**

| | Volta Phase Plate | Defocus |
|---|---|---|
| Microscope | Titan Krios G1 | |
| Magnification | 42,000 | |
| Voltage (kV) | 300 | |
| Electron exposure ($e^-/Å^2$) | ~100-120 | |
| Detector | Gatan K2 Summit | |
| Energy filter | Yes | |
| Slit width (eV) | 20 | |
| Phase plate | Yes | No |
| Defocus range (μm) | -0.5 | -3.25 to -5 |
| Tilt range (min/max, starting angle, step) | -50/70°, 10°, 2° | |
| Tilt scheme | Unidirectional | Dose-symmetric |
| Pixel size (Å) | 3.42 | |
| Tomograms (no.) | 3 | 10 |
| Cells (no.) | 1 | 7 |
| Tomograms (no.) used for packing analysis/Cells (no.) | 3/1 | 6/4 |
| Tomograms (no.) used for averaging and polarity assessment/Cells (no.) | - | 10/7 |

**Supplementary Table 2 | Data processing parameters**

| | Cardiac actin-Tpm filament in the myosin state (EMD-11826) | Cardiac actin-Tpm filament in an intermediate state (EMD-11825) |
|---|---|---|
| Pixel size (Å) | 3.42 | 3.42 |
| Subtomograms (no.) | 56,858 | 27,030 |
| Tomograms (no.)/Cells (no.) | 2/2 | 1/1 |
| Symmetry imposed | C1 | C1 |
| FSC threshold | 0.143 | 0.143 |
| Map resolution (Å) | 15.7 | 17.7 |